J Fluoresc (2008) 18:867–876
DOI 10.1007/s10895-008-0316-3

ORIGINAL PAPER

Competitive FRET-Aptamer-Based Detection of Methylphosphonic Acid, a Common Nerve Agent Metabolite

John G. Bruno · Maria P. Carrillo · Taylor Phillips · Neal K. Vail · Douglas Hanson

Received: 8 October 2007 / Accepted: 2 January 2008 / Published online: 26 January 2008

Abstract Competitive fluorescence resonance energy transfer (FRET)-aptamer-based assay formats are described for one-step detection of methylphosphonic acid (MPA; a metabolite of several organophosphorus (OP) nerve agents). AminoMPA was attached to tosyl-magnetic beads and used for DNA aptamer selection from which one dominant aptamer sequence emerged. Two different FRET approaches were attempted. In one approach, the complementary DNA sequence was used as a template for labeling the aptamer with Alexa Fluor 546 (AF 546)-14-dUTP by asymmetric PCR. Following 3-dimensional (3-D), molecular modeling of the aptamer-MPA complex, a series of three fluoresceinated aptamers labeled at positions 50, 51, and 52 in the putative optimal binding pocket were synthesized. In both FRET formats, aminoMPA was linked to Black Hole Quencher (BHQ-1 or BHQ-2)-succinimides and allowed to bind the fluorescein or AF 546-labeled MPA aptamer. Following gel filtration to purify the labeled MPA aptamer-BHQ-aminoMPA FRET complexes, the complexes were competed against various concentrations of unlabeled MPA, MPA derivatives, and unrelated compounds in titration and cross-reactivity studies. Both approaches yielded low microgram per milliliter detection limits for MPA with generally low levels of cross-reactivity for unrelated compounds. However, the data suggest a pattern of traits that may effect the direction (lights on or off) and intensity of the FRET.

Keywords Aptamer · Asymmetric PCR · Fluorescence resonance energy transfer · Organophosphorus · SELEX

J. G. Bruno (✉) · M. P. Carrillo · T. Phillips
Operational Technologies Corporation,
4100 NW Loop 410, Suite 230,
San Antonio, TX 78229, USA
e-mail: john.bruno@otcorp.com

N. K. Vail · D. Hanson
Chemistry and Chemical Engineering Division,
Southwest Research Institute,
6220 Culebra Road,
San Antonio, TX 78228, USA

Introduction

It is an unfortunate but modern reality that some nations must be vigilant against chemical and biological (CB) attacks. Early detection of CB attacks can be crucial to proper patient treatment and subsequent accurate forensics. At present, laboratory-bound techniques such as high-performance liquid chromatography (HPLC) and gas chromatographic-mass spectrometry (GC-MS) provide the standard instruments and methods to detect and identify nerve agents or their metabolites especially in body fluids [1]. Portable and rapid field detection and identification of these analytes is desirable for screening purposes and to augment the standard laboratory methods.

In the cases of sarin (GB), soman (GD), and VX, hydrolysis products include methylphosphonic acid (MPA) and its various derivatives such as isopropyl methylphosphonic acid (IPMPA) and pinacolyl methylphosphonic acid (PMPA). Therefore, we sought to develop a one-step (bind and detect) fluorescence assay for MPA, the common portion of these analytes, using a novel competitive FRET-aptamer approach. A number of attempts to develop high affinity antibodies against nerve agents or their analogs have met with limited success [2–4]. In this work, we report the first attempt to develop an aptamer to a component of OP nerve agents.

Although SELEX (Systematic Evolution of Ligands by EXponential enrichment) has been used to develop aptamers against small molecules [5–7], MPA is extremely small, consisting of only 10 atoms in its protonated state.

Hence, we were reluctant to attempt aptamer development to such a small molecule. However, Mann et al. [6] published a compelling report concerning DNA aptamer development against the comparably small molecule ethanolamine with K_d values ranging from 6 to 19 nM using a magnetic bead (MB)-based selection methodology similar to our own [8]. These facts, coupled with the commercial availability of aminoMPA for simple coupling to tosyl-MBs, made the project appear feasible.

The use of FRET or changes in fluorescence intensity to mark aptamer-analyte binding events has been described with a number of variations. Investigators have labeled aptamers with fluorophores (F) and quenchers (Q) in various ways [9–15] or fluorophore-labeled aptamers without using a recognized quencher at all [10, 14] and still achieved low levels of detection. In our scheme, which was based on previous competitive antibody FRET [16], the analyte is first labeled with a known Q, then allowed to bind and complex with an F-labeled aptamer. The aptamer can be singly labeled internally during solid-phase synthesis or multiply labeled internally by asymmetric PCR using F-labeled deoxynucleotides and the aptamer's complementary DNA as a template to produce single-stranded F-labeled aptamers [17–19]. The F-labeled aptamer-Q-ligand complex is then purified by gel filtration over Sephadex™ and the complex is identified in the fraction or fractions demonstrating the highest simultaneous absorbance for DNA, the analyte, F, and Q at their respective peak absorbance wavelengths. The FRET-aptamer-Q-target complex is then diluted and used in competition with unlabeled target analyte (Fig. 3) to develop FRET titration curves as demonstrated in the present work.

Experimental

Oligonucleotides, fluorophores, quenchers, and other chemicals

All oligonucleotides were obtained from Integrated DNA Technologies, Inc. (IDT; Coralville, IA). The SELEX template sequence was: 5′-ATCCGTCACACCTGCTCT-N_{36}-TGGTGTTGGCTCCCGTAT-3′, where N_{36} represents the randomized 36-base region of the DNA library. Primer sequences were: 5′-ATACGGGAGCCAACACCA-3′ (designated forward) and 5′-ATCCGTCACACCTGCTCT-3′ (designated reverse) to prime the template and nascent strands respectively. AF 546-14-dUTP was obtained from Invitrogen, Inc. (Carlsbad, CA) at 1 mM in TE buffer. BHQ-1-succinimide and BHQ-2-succinimide esters were obtained from Biosearch Technologies, Inc. (Novato, CA). MPA, isopropyl methylphosphonic acid (IPMPA), diisopropyl MPA (Di-IPMPA), cyclohexyl MPA (CH-MPA), ethyl MPA (E-MPA), and pinacolyl-MPA (PMPA), were obtained from Cerilliant, Corp. (Round Rock, TX) at a concentration of 1 mg/ml in methanol. A previously described para-aminophenyl-soman derivative [2–4] was obtained from the US Army Medical Research Institute for Chemical Defense (USAMRICD), Aberdeen Proving Ground, MD. AminoMPA and all other chemicals were obtained from Sigma-Aldrich Co. (St. Louis, MO).

SELEX aptamer development, cloning, and sequencing, and secondary structure determinations

AminoMPA was attached to tosyl-M280 MBs (Invitrogen Corp.) by incubation of 100 μl of tosyl-M280 MBs (approximately 2×10^8 MBs) with 1 mg/ml of aminoMPA overnight at 37 °C. AminoMPA-MBs were collected and washed 3 times in 1 ml of 1× SELEX binding buffer (1×BB; 0.5 M NaCl, 10 mM Tris–HCl, and 1 mM $MgCl_2$, pH 7.5–7.6) using a Dynal MPC-S magnetic collector. Five rounds of SELEX were performed as previously described [8] using the 72 base library and primers described above. *E. coli* single-stranded binding protein (SSB, 0.5 U) in the form of Perfect Match® from Statagene, Corp. (La Jolla, CA) was added to every PCR reaction to avoid higher molecular weight concatamers of the aptamers and produce a single 72-bp band on electrophoretic gels [20]. Following five rounds of SELEX, the selected aptamer population was cloned into pCR II TOPO plasmids using the Invitrogen TOPO TA Cloning Kit with dual promoters. Plasmids were transfected into chemically competent TOP10F' *E. coli*. White colonies were selected from antibiotic-supplemented media and the plasmids containing aptamer inserts were extracted using a SNAP™ kit (Invitrogen) and sent to SeqWright, Inc. (Houston, TX) for sequencing. Secondary structures were determined over a range of temperatures from 4 °C to 37 °C using the Internet software program "Vienna RNA" [21] from the Institute for Theoretical Chemistry, University of Vienna, Austria; http://rna.tbi.univie.ac.at/cgi-bin/RNAfold.cgi using RNA and DNA parameters [22] as appropriate (Fig. 3).

3-D molecular modeling and MPA binding simulations

Aptamer and MPA models were constructed using Materials Studio Visualizer (Accelrys Software, Inc., Valencia, CA, V2.2). The structures were optimized with a combination of molecular mechanics and molecular dynamics using Discover software and a Consistent-Valence Force Field (CVFF), which is suitable for studying peptides, proteins, and wide variety of organic systems.

The aptamer model was built in segments of five to ten nucleotides to correspond with key features of the full structure. After adding each segment, the resulting structure was then energy minimized by molecular mechanics. Minimization was conducted for at least 5,000 iterations

and used a smart minimization algorithm with a final convergence criteria of 0.1 kcal mol^{-1} $Å^{-1}$. After the final structure was energy minimized, it was relaxed by molecular dynamics at an elevated temperature, then annealed at progressively cooler temperatures until achieving a system temperature of 25 °C. Relaxation and annealing were conducted for at least 50 ps using a time step of 1 fs. Similar methods were used to construct MPA.

Six optimized MPA molecules were added to the optimized polynucleotide. Three MPA molecules were located in probable binding sites designated MPA2, MPA4, and MPA6. The remaining MPA molecules were placed in "control" sites designated MPA 1, MPA3, and MPA5. These latter sites were chosen to provide comparisons with the MPA6 site, an exterior "fold" and a linear segment distal from a "bend" in the DNA. The composite aptamer-MPA structure was energy minimized by molecular mechanics and relaxed using molecular dynamics according to published methods [23]. Total system energy stabilized at approximately −6,000 kcal/mol.

Once the composite structure was fully relaxed, five random conformers were generated using additional dynamics runs. Binding energies (E) were calculated for each conformer and each MPA molecule by the following equation:

$$\text{E Binding} = \text{E Total} - [\text{E Aptamer(Without MPA)} + \text{E MPA Only}]$$

Fluorophore labeling of MPA aptamer by asymmetric PCR and during solid-phase synthesis

Once a dominant MPA aptamer sequence had been identified (see "Results" for aptamer sequence), its complementary DNA (cDNA) was synthesized and obtained from IDT for use as a template for asymmetric PCR involving a 100:1 reverse: forward primer ratio. The asymmetric PCR reaction was doped with 4 μM AF 546-14-dUTP and contained 224 pmol of aptamer cDNA along with 1 μl of rTaq (5 U/μl, TakaRa, Otsu, Shiga, Japan) in EasyStart Micro 100™ pre-made PCR mix tubes (Molecular BioProducts, Inc., San Diego, CA). Ten microliters of 10× PCR buffer (TakaRa) and sufficient nuclease-free deionized water were added to bring the final volume of each PCR tube to 100 μl. PCR was conducted under the following conditions: 95 °C for 5 min, 30 cycles of 95 °C for 30 s, 53 °C for 30 s and 72 °C for 30 s, followed by a 7 min extension period at 72 °C and storage at 4 °C.

In the alternate assay approach, three separate aptamers were singly fluorescein labeled by IDT using fluorescein-C6 linker-dTTP during solid-phase synthesis. The aptamers were labeled with fluorescein at nucleotides 50, 51, and 52 (numbered from the 5′ end) and designated accordingly as 50F, 51F, and 52F. They were reconstituted in 1X BB at a stock concentration of 0.2 mg/ml.

Generation of quencher-ligands, complexation, and purification of FRET reagents

BHQ-1- or BHQ-2-succinimide esters were dissolved in dimethylsulfoxide at 1 mg/ml. Three hundred μl of BHQ-2-succinimide were added to 300 μl of 1 mg/ml aminoMPA in 2XBB and briefly mixed. The solution was incubated at 37 °C overnight and subsequently referred to as the "Q-ligand." Two hundred μl of Q-ligand solution were added to 200 μl of fluorescein or AF-546-dUTP-labeled MPA aptamers and allowed to bind for at least 20 min at room temperature (RT). Next, the AF 546-aptamer-Q-ligand complexes were purified by passage over a 1XBB-equilibrated PD-10 (Sephadex™ G-25, G.E. Healthcare, Inc., Piscataway, NJ) gel filtration column. One ml fractions were collected using 1XBB and the absorbance of each fraction at 260, 495, and 540 or 555 and 579 nm (representing peak absorbances for DNA, fluorescein and BHQ-1 or AF 546 and BHQ-2 respectively) were used to assess which fractions would be used for FRET experiments (i.e., which fractions contained the F-aptamer-Q-ligand complexes).

Spectrofluorometric assessment

Competitive FRET assays and cross-reactivity studies were set up so that 20 μl of the AF 546-aptamer-Q-ligand complex (approximately 0.7 to 1.2 μg of FRET-aptamers) were added to methacrylate cuvettes containing serial two-fold dilutions of MPA or other compounds of interest in 1XBB. Similar competitive FRET-aptamer assay titrations were set up for the fluorescein-labeled aptamers (i.e., 50F–52F) except that approximately 6.7 μg of labeled aptamers were used per cuvette. All cuvettes were brought to a final volume of 2 ml using 1×BB and allowed to equilibrate at RT for at least 20 min. Fluorescence spectra were acquired with a Varian, Inc. (Palo Alto, CA) Cary Eclipse spectrofluorometer using an excitation of 495 nm for fluorescein or 555 nm for AF 546 and scanning from 500–600 or 550–650 nm with 5 nm excitation and emission slit widths, medium scanning speed, 1 nm resolution, and 600 or 900 V photomultiplier (PMT) voltage. The fluorescein-based experiments used 600 V and the AF 546-based experiments used 900 V PMT settings.

Results

MPA aptamer sequence and conventional fluorescence assessment of aptamer binding

Several of the clones sent to SeqWright revealed evidence of partial or complete aptamer inserts. Two potential

aptamer sequences designated MPA1 and MPA2 dominated the pool and these were verified to be complementary in the double-stranded plasmid. To determine which sequence was truly the MPA-binding aptamer, we obtained 5′-fluoresceinated MPA1 and MPA2 sequences from IDT, attempted to bind these to aminoMPA-MBs and washed the beads three times in 1XBB. The 5′-fluoresceinated aptamer-aminoMPA-MBs were resuspended immediately prior to analysis in the Eclipse spectrofluorometer. The resultant readings demonstrated approximately 10-fold greater fluorescence intensity from the MPA2 sequence versus the MPA1 sequence (data not shown). Hence, the oligonucleotide designated MPA2 (5′-ATCCGTCACACCTGCTCT-CGATGAGACAAGAGGAACACGGCACAATTGATT TAA-TGGTGTTGGCTCCCGTAT-3′) was considered to be the true aptamer for subsequent experiments.

Aptamer secondary structure and 3-D modeling of the aptamer-MPA complex

The MPA2 DNA sequence was subjected to secondary structural analyses using web-based Vienna RNA software [21] with RNA or DNA parameters [22] as appropriate at 25 °C as shown in Figs. 1 and 3. Three-dimensional (3-D) modeling also revealed a convoluted aptamer structure (Fig. 1a) with several potential binding sites for MPA. The site designated MPA6 appeared to have the greatest negative free energy change upon binding MPA (−113.6 kcal/mol as shown in Fig. 1b). Despite the very small size of MPA, several types of forces including hydrogen bonds and van der Waals interactions appear to play a significant role in enabling and stabilizing binding of MPA to the aptamer in particular at the MPA6 site.

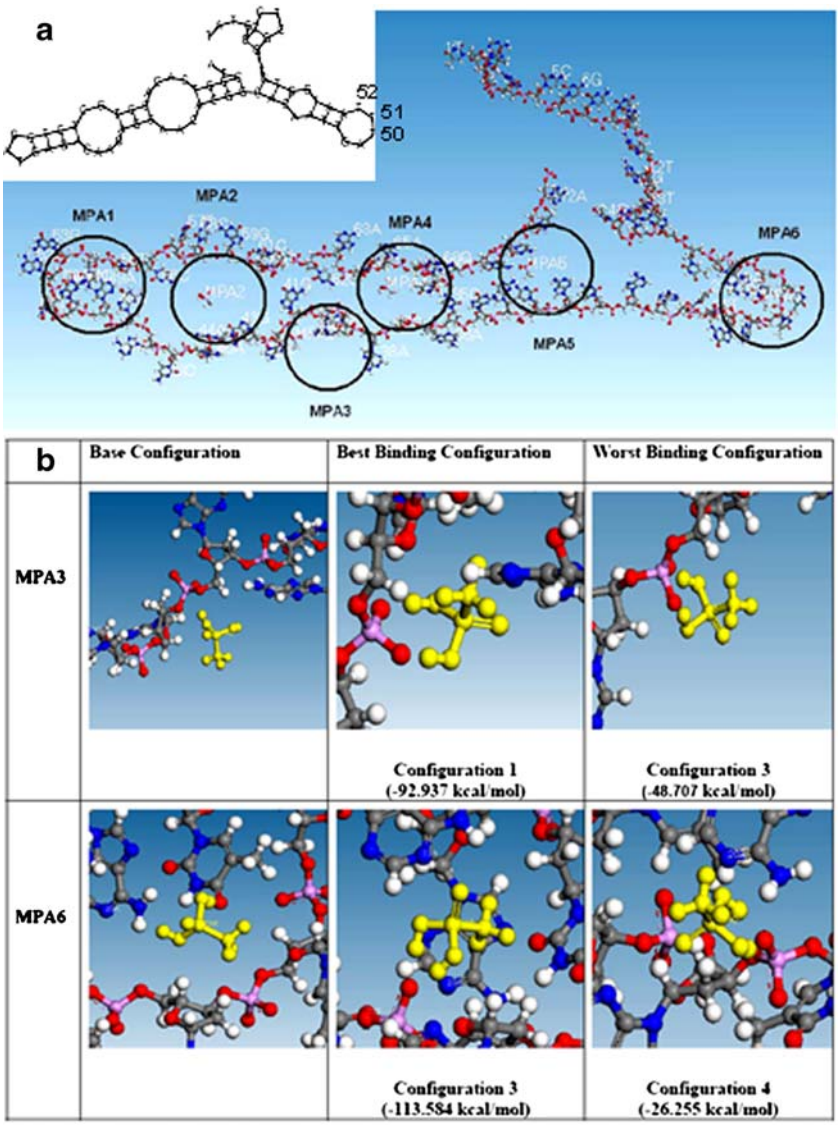

Fig. 1 **a** Secondary structure of the MPA2 aptamer at 25 °C as predicted by web-based Vienna RNA software using DNA parameters and the 3-D structure predicted by computer modeling showing possible binding sites for MPA. **b** Close up views of the two most probable binding sites in their best (lowest energy) and worst (highest energy) configurations

Evidence of successful Alexa Fluor 546-dUTP labeling of the MPA aptamer and FRET-aptamer purification

Successful asymmetric PCR-based incorporation of AF 546-14-dUTP was expected because of the relatively long (14-atom) linker arm which allows DNA polymerases to incorporate AF 546-14-dUTP in a relatively unhindered manner [18, 19]. The image of an unstained Tris Borate EDTA (TBE)-polyacrylamide electrophoresis gel on the left side of Fig. 2 demonstrates that AF 546-14-dUTP was incorporated into the 72 bp aptamer by asymmetric PCR because a crisp fluorescent band is observed. Subsequent ethidium bromide staining of the same gel reveals that the fluorescent bands across the gel fall between the 50 and 100 bp markers on the now visible DNA ladder, making them of the correct size to be the AF 546-labeled aptamers.

Since AF 546-14-dUTP was used to dope the nascent aptamer population, one can predict all the potential sites where a fluorophore might reside in the MPA2 aptamer, because some or all of the thymine bases will be replaced by the fluorophore-labeled dUTPs (underlined uridines in Figs. 2 and 3). AF 546-14-dUTP could not incorporate into the 18 bases nearest the 5′ end of the nascent MPA aptamer because asymmetric PCR was used and this portion of the new strand is accounted for by unlabeled primer incorporation into the new strand. The uridines or thymines at positions 50–52 correspond to nucleotides in the putative MPA6 binding site as shown in Fig. 1a. Therefore, the combination of asymmetric PCR dUTP incorporation data with 2-D and 3-D modeling proved highly useful for determining a likely locus to place fluorophores in the MPA structure to minimize the number of fluorophores while maximizing FRET potential.

Fractions 5–7 from the Sephadex G25 column were deemed to be optimal for FRET assays because they contained the highest absorbances at 260 nm for DNA aptamers, 495 nm for fluorescein, and 540 nm for BHQ-1-aminoMPA ligand bound to the fluorescein-labeled aptamers (data not shown). Similarly, fractions 5–7 from the AF 546-dUTP asymmetric PCR-labeled population were collected and pooled for competitive FRET assays because they exhibited the highest absorbance for DNA at 260 nm along with the highest absorbance at 555 nm for AF 546-dUTP and 579 nm for BHQ-2-labeled aminoMPA ligand complexed to the fluorophore-labeled MPA aptamer (data not shown).

Spectrofluorometric results of MPA titration with the AF 546 asymmetric PCR-labeled system

Figure 4a demonstrates a typical “lights on” FRET response for the asymmetric PCR-labeled system using overlying fluorescence emission spectra for the competitive assay in varied concentrations of MPA from 0 to 250 μg/ml. The same general FRET response trend was noted again in Fig. 4b with some smaller doses of MPA, but higher background fluorescence from a second batch of FRET reagent (i.e., AF 546-doped aptamer complexed to BHQ-2-amino MPA). In Fig. 4c, the asymmetric PCR-labeled aptamer-ligand complex competitive FRET system was

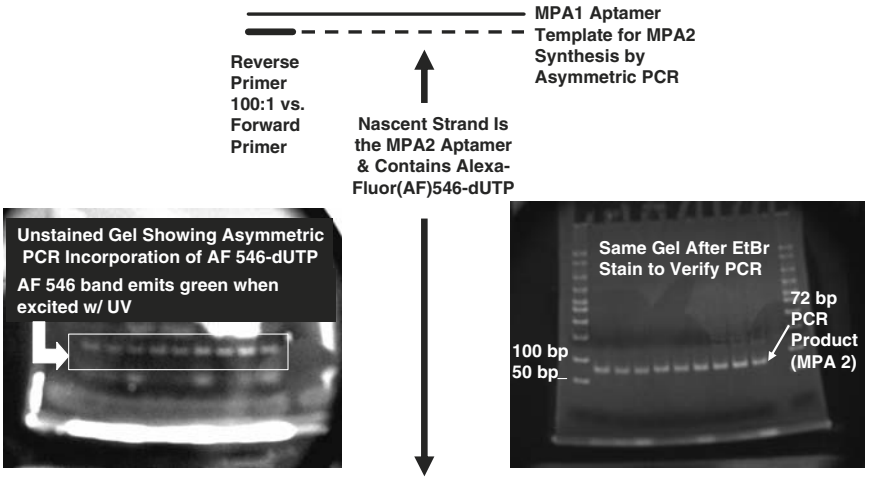

Fig. 2 Electrophoresis data for the asymmetric PCR-based doping of the MPA aptamer (designated MPA2) using its complementary DNA template. The gel images demonstrate the appearance of an unstained 4–20% Tris-polyacrylamide gradient gel (*left*) with the AF 546-14-dUTP-labeled aptamers after asymmetric PCR and the appearance of the same gel after ethidium bromide (*EtBr*) staining (*right*) to reveal the DNA ladder and that the unstained fluorescent bands are truly composed of DNA (*right*). Below the gel images, the cDNA template (MPA1) sequence and the nascent strand (MPA2 aptamer) sequence with all potential AF 546-14-dUTP incorporation sites (marked as *underlined* uridines) are given

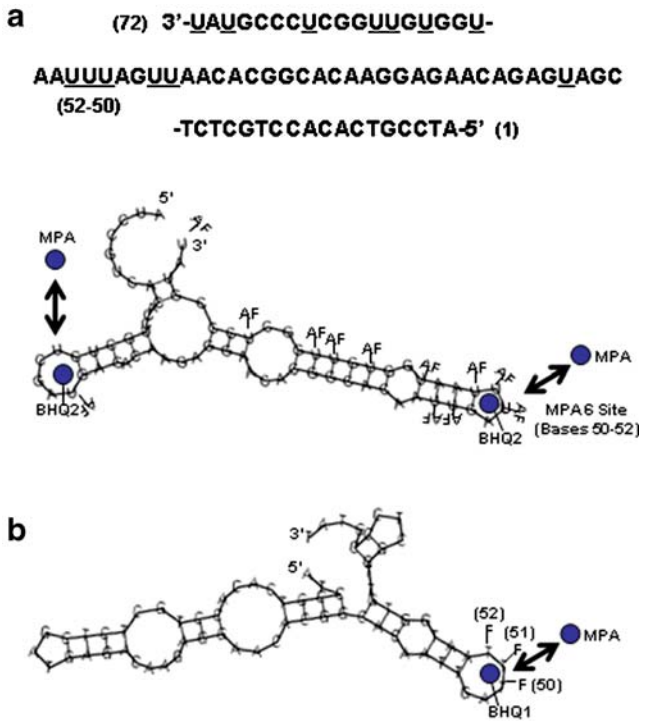

Fig. 3 Conceptual diagrams of the two competitive FRET systems employed. **a** Illustration of the asymmetric PCR AF 546 system showing the positions of all possible AF 546 labels and potential binding pockets for competitive FRET between BHQ-2-labeled MPA and unlabeled MPA from a test sample. This aptamer was folded using RNA parameters in the Vienna RNA software, because of the AF 546-dUTP incorporation. No uridines actually exist in the first 18 bases from the 5′ end, therefore no AF is shown attached to them. **b** The singly fluorescein-labeled competitive FRET system in which BHQ-1-MPA is competed against unlabeled MPA. This system demonstrated a "lights off" response to increasing concentrations of unlabeled MPA, possibly by BHQ-1 or MPA-mediated quenching of fluorescein from the bulk solution [30, 31]. This aptamer was folded using DNA parameters [22] by Vienna RNA software

shown to be highly reproducible within a given batch because three independent spectra lay directly on top of one another for each concentration of MPA examined. Regardless of batch variation or background fluorescence, both assay attempts produced a sensitivity limit of approximately 8–10 μg of MPA per milliliter.

Cross-reactivity of the AF 546-asymmetric PCR-labeled system

The AF-546-labeled competitive FRET-aptamer assay was also conducted with equimolar concentrations (52 μM) of MPA, IPMPA, PMPA, and aminoMPA to test the effects of structurally similar analytes on the assay. As Fig. 5a reveals, addition of IPMPA and PMPA yielded virtually the same fluorescence increase as an equal amount of MPA itself, suggesting that the aptamer binds the MPA portion of the targets and is probably not sterically hindered by the isopropyl or pinacolyl groups. In Fig. 5b, we examined cross-reactivity of the FRET assay using comparable molar amounts of the unrelated analytes triethylamine and Tris–HCl [tris-(hydroxymethol)aminomethane-hydrochloride], which did not alter the pH. These compounds had very little effect on the baseline fluorescence spectrum of the assay. However, an equimolar amount of aminoMPA appeared to decrease the fluorescence response as shown in Fig. 5b. This "lights off" response from aminoMPA

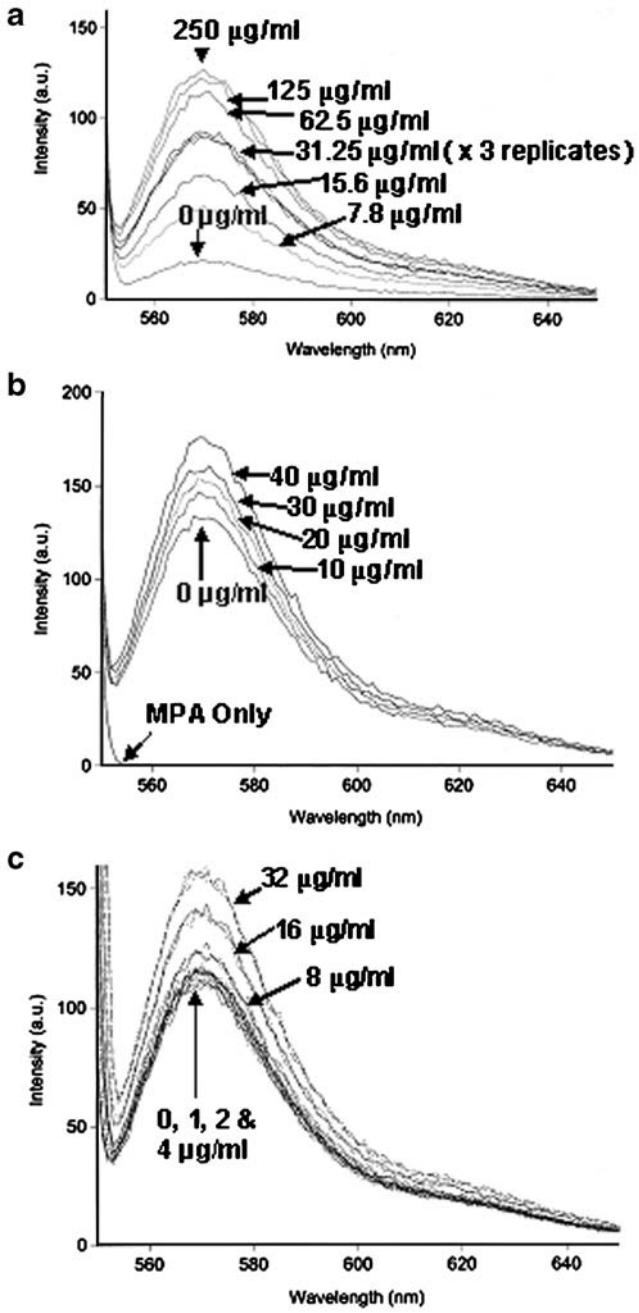

Fig. 4 Results of competitive FRET-aptamer experiments using two different batches (**a**, **b**) of AF 546-dUTP asymmetric PCR-labeled aptamer complexed to BHQ-2-aminoMPA and competed with varying levels of unlabeled MPA. **c** Competitive FRET-aptamer reproducibility study of MPA detection using this system

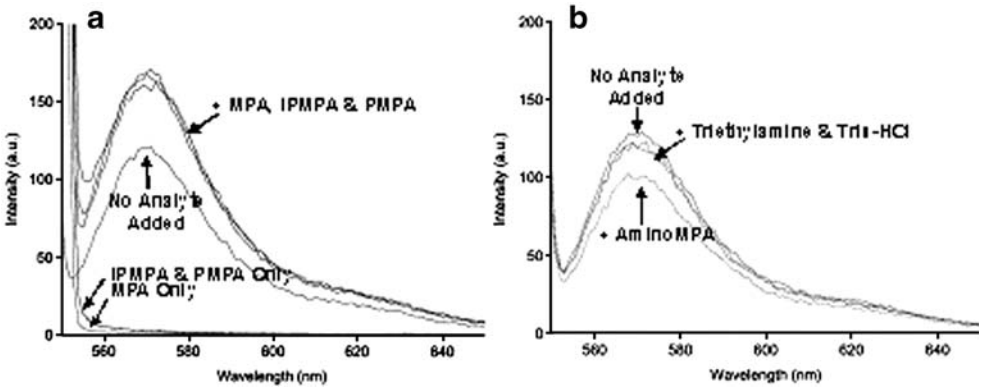

Fig. 5 Results of two cross-reactivity studies for the PCR-labeled AF 546 MPA aptamer system. Subpanel **a** shows the FRET response to addition of MPA at 50 μg/ml and equal molar amounts (52 μM) of IPMPA and PMPA versus the background fluorescence spectrum of the FRET complex reagent alone (no analyte added). Also indicated are the negligible fluorescence spectra of 50 μg/ml of MPA, IPMPA and PMPA alone without any FRET reagent complex added. Subpanel **b** illustrates the FRET response of equal molar amounts (52 μM) of aminoMPA, triethylamine, and Tris–HCl

could be due to binding and an electrostatic interaction between the amino group of aminoMPA and the AF 546-labeled aptamer. Examination of the chemical structure of AF 546-14-dUTP reveals several sulfite and carboxyl groups that would be available to attract amino-MPA. Regardless of the mechanism, the aminoMPA FRET result again illustrates some degree of specificity or change in fluorescence due to a compound that is structurally related to MPA. If the decreased fluorescence effect had only been due to the nonspecific addition of an amine compound, then both triethylamine and Tris–HCl might be expected to alter the fluorescence response, but this effect was only observed with aminoMPA, suggesting a specific binding pocket interaction between aminoMPA and the AF 546-labeled aptamer.

Spectrofluorometric results of MPA titration with the fluorescein-labeled systems

Results of two-fold MPA titrations on FRET from the 50F, 51F, and 52F aptamers as well as a reproducibility study are given in Fig. 6. The singly fluorescein-labeled systems yielded detection limits comparable to the multiple AF 546-dUTP asymmetric PCR-labeled system (low μg per ml levels of MPA). However, in contrast to the AF 546 system, the fluorescein-labeled systems all gave "lights off" responses to increasing levels of MPA. Figures 6a and c reveal that the 50F aptamer gave the best overall separation of scans with a detection limit of 12.5 μg of MPA per ml and highly reproducible results (Fig. 6c). The 51F and 52F aptamers also responded to MPA, but with sensitivities closer to 25–50 μg of MPA per ml. Since FRET capacity appeared to decline from 50F to 52F, it appears that the real FRET effect may be centered around nucleotide 50 (i.e., nucleotide 50 is well within the Förster distance). Many of the spectra are too close to discriminate in Fig. 6, so ranges of MPA concentrations corresponding to the spectra are indicated by brackets.

Cross-reactivity of the fluorescein-labeled systems

In an attempt to further characterize the nature of the putative MPA6 binding pocket in the optimal aptamer from Fig. 6, we also investigated cross-reactivity of the 50F aptamer with MPA-related and unrelated ligands. Figure 7 summarizes the results of this cross-reactivity study and reveals several trends. Diisopropyl MPA (Di-IPMPA) gave a slight enhancement of the fluorescence, while the rank order of decreasing fluorescence was: cyclohexyl MPA (CH-MPA) ≈ pinacolyl MPA (PMPA) > isopropyl MPA (IPMPA) ≈ ethyl MPA (E-MPA) > MPA > aminoMPA. Other related (e.g., para-amino-phenyl soman (p-AP-soman)) and unrelated compounds such as acetylcholine (ACh) and bovine serum albumin (BSA) caused little, if any change in fluorescence of 50F. Oddly, triethylamine, which had no effect on the AF 546 asymmetric PCR-labeled aptamer, demonstrated a fluorescence enhancement of the 50F system. Finally, aminoMPA led to nearly complete quenching of the 50F fluorescein-labeled system. Similar trends in cross-reactivity and FRET behavior were noted in subsequent analyses of the 51F and 52F systems (data not shown for brevity).

Discussion

The results presented here validate a novel competitive FRET-aptamer assay platform approach which involves incorporation of fluorophores into DNA aptamers via asymmetric PCR followed by complexation to quencher-

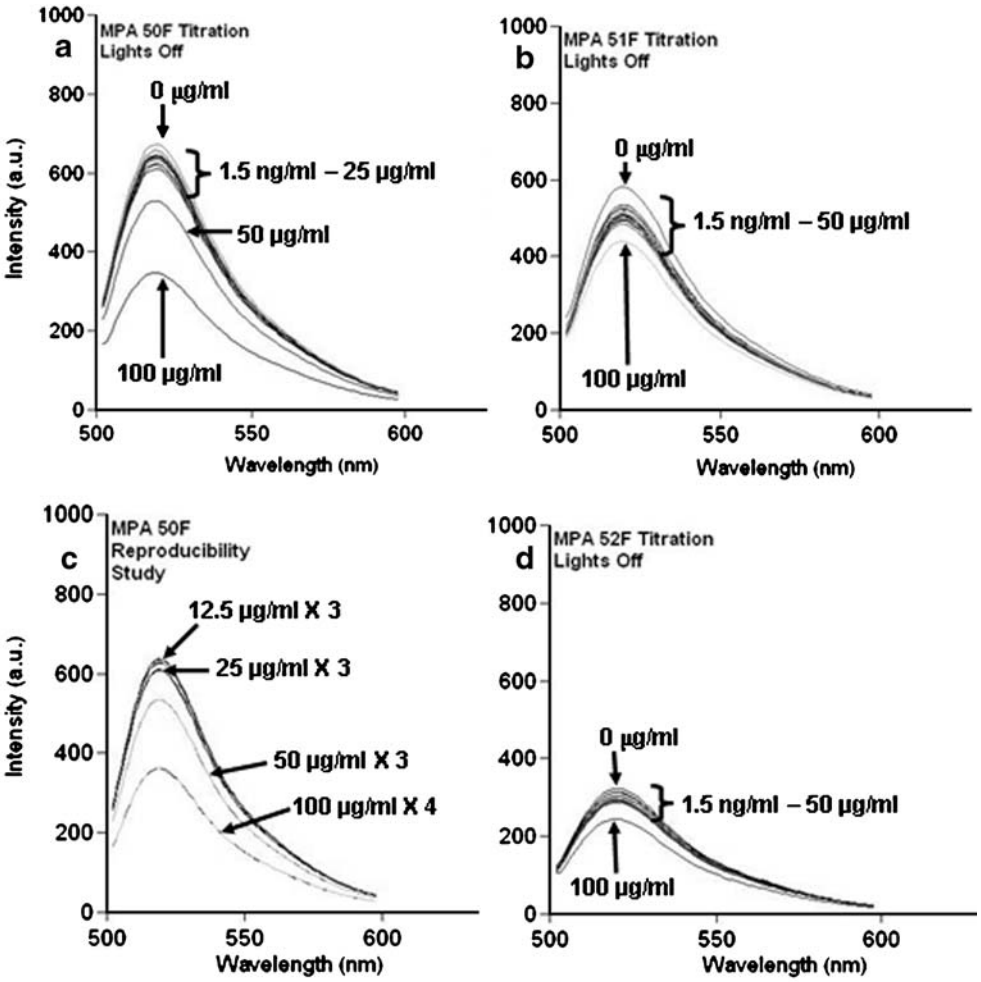

Fig. 6 FRET spectra for MPA titration of the three fluorescein-labeled MPA aptamers (**a**, **b** and **d**). Subpanel **c** represents a reproducibility study for the MPA 50F aptamer system with the indicated number of replicate spectra for each MPA concentration

labeled ligands and simple gel filtration-based purification of FRET reagent complexes. The FRET reagent complexes can then be competed with unlabeled analytes to enable rapid, homogeneous, and highly reproducible detection.

Neither the aptamer system labeled with fluorescein during solid-phase synthesis nor the asymmetric PCR-labeled system were ultrasensitive to MPA. This may be a reflection of the relatively high affinity of the aptamer predicted by computer modeling. Higher affinity aptamers may not be expected to allow competitive displacement of their cognate targets, because they bind tightly to the Q-labeled target and rarely release it. We investigated the single fluorescein-labeled aptamers, because we thought that multiple fluorophores in the PCR-labeled system were contributing to high background and diminishing signal-to-noise ratio, thereby decreasing assay sensitivity. However, that does not appear to be true, because both systems gave comparable low microgram per milliliter detection limits for MPA. In the case of the heavily PCR-labeled AF 546 aptamer system, the multiple fluorophores appear to be quite close to one another (Figs. 2 and 3a) and therefore may actually self-quench [24–27].

Regardless, of the assay's ultimate sensitivity, specificity, or utility, the MPA aptamer-MPA combination served as a useful FRET model system for studying DNA interactions with very small molecules. Surprisingly, the systems studied revealed that both "lights on" and "lights off"

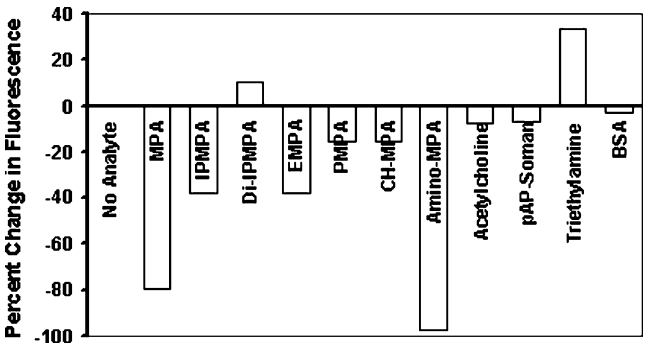

Fig. 7 FRET results of cross-reactivity studies for the MPA 50F aptamer. All ligands were added at 100 µg per sample. *ACh* Acetylcholine, *BSA* bovine serum albumin, *CHMPA* cyclohexyl-MPA, *EMPA* ethyl-MPA, *IPMPA* isopropyl-MPA, *Di-IPMPA* diisopropyl-MPA, *p-AP-soman* para-aminophenyl-soman, and *PMPA* pinacolyl-MPA. Similar results were obtained with the 51F and 52F aptamers (data not shown)

responses could be elicited from the same aptamer, if variously decorated with fluorophores and associated quenchers. We speculate that the general "lights on" response of the PCR-labeled AF 546 system may be due to multiple fluorophores and multiple potential binding pockets in the aptamer structure which lead to a net increase in light output. Conversely, it appears that the MPA6 binding pocket is primarily capable of a "lights off" response which is centered around nucleotide position 50.

In theory, there are only two means to produce a "lights off" response in our competitive FRET-aptamer systems (Fig. 3). One way is for the aptamer to undergo a conformational change when the Q-labeled target is released and the fluorophore or fluorophores become more fully quenched by the DNA itself [28, 29]. However, this seems unlikely in the present systems, because the BHQ dyes are more efficient quenchers than natural nucleotides [30]. The other mechanism is for Q-MPA conjugates to associate with the aptamer-bound fluorophores (i.e., make contact within the Förster distance) after Q-MPA is released into the bulk solution. Upon initial consideration, this may seem unlikely in bulk solution. However, Marras et al. [30] report that both BHQ-1 and BHQ-2 exhibited noteworthy affinity for AF 546 and carboxyfluorescein in hybridization studies in which the F–Q interactions elevated the melting temperatures of labeled DNA hybrids 5–6 °C versus that of unlabeled DNA hybrids. It is also possible that electrostatic repulsion between the negatively charged MPA, which is ionized at neutral pH [31], and the negatively charged fluorescein or AF 546 could be neutralized by the divalent Mg^{2+} cations in our 1XBB buffer system, thereby facilitating contact-mediated quenching in solution [30]. In addition, MPA itself may actually be a quencher of some fluorescent dyes, because Heleg-Shabtai et al. [31] observed significant effects of MPA on the fluorescence of eosin, which is structurally similar to fluorescein.

The cross reactivity studies were also enlightening in that they demonstrated differential responses of the two FRET systems to the same ligands such as triethylamine (compare Figs. 5 and 7). In addition, it appeared clear that larger hydrophobic groups (e.g., isopropyl, diisopropyl, or cyclohexyl groups) attached to MPA did not decrease fluorescence as much as MPA or aminoMPA (Fig. 7). We can only speculate about this finding at present, but again several potential hypotheses exist. Perhaps, by physically widening the binding pocket with the larger hydrophobic groups, light output was somewhat more enabled. It is also possible that nonspecific quenching by the analytes [31] or changes in aptamer conformation induced by binding of related analytes led to quenching by nucleotides in the DNA itself [28–29], which are less effective quenchers than the BHQ dyes [30]. If multiple binding sites exist in an aptamer, it may also be possible that "allosteric" effects on conformation exist which could effect the orientation of fluorophores and the net light output.

Corry et al. [32] and Hofkens [26] have attempted to model complex 3-D FRET systems such as those described herein involving multiple binding sites, fluorophores and quenchers. While the algorithms Corry et al. [32] have developed are highly useful for FRET predictions, our actual experiments with two different competitive FRET systems illustrate the ultimate value of empiricism in demonstrating the direction of FRET behavior (i.e., determining "lights on or off") in a complex system.

Acknowledgments This work was supported by the US Army under Contract Nos. W81XWH-06-C-0366 and W911SR-06-C-0059.

References

1. Driskell WJ, Shih M, Needham LL, Barr DB (2002) Quantitation of organophosphorus nerve agent metabolites in human urine using isotope dilution gas chromatography-tandem mass spectrometry. J Anal Toxicol 26:6–10
2. Glikson M, Arad-Yellin R, Ghozi M, Raveh L, Green B, Eshkar Z (1992) Characterization of soman-binding antibodies raised against soman analogs. Molec Immunol 29:903–910
3. Brimfield AA, Hunter KW, Lenz DE, Benschop HP, Van Dijk C, De Jong LPA (1985) Structural and stereochemical specificity of mouse monoclonal antibodies to the organophosphorus cholinesterase inhibitor soman. Mol Pharmacol 28:32–39
4. Johnson JK, Cerasoli DM, Lenz DE (2005) Role of immunogen design in induction of soman-specific monoclonal antibodies. Immunol Lett 96:121–127
5. Jenison RD, Gill SC, Pardi A, Polisky B (1994) High-resolution molecular discrimination by RNA. Science 263:1425–1429
6. Mann D, Reinemann C, Stoltenberg R, Strehlitz B (2005) *In vitro* selection of DNA aptamers binding ethanolamine. Biochem Biophys Res Comm 338:1928–1934
7. Stojanovic MN, de Prada P, Landry DW (2001) Aptamer-based folding fluorescent sensor for cocaine. J Am Chem Soc 123:4928–4931
8. Bruno JG, Kiel JL (2002) Use of magnetic beads in selection and detection of biotoxin aptamers by ECL and enzymatic methods. BioTechniques 32:178–183
9. Hamaguchi N, Ellington A, Stanton M (2001) Aptamer beacons for the direct detection of proteins. Anal Biochem 294:126–131
10. Jhaveri S, Rajendran M, Ellington AD (2000) *In vitro* selection of signaling aptamers. Nature Biotechnol 18:1293–1297
11. Katilius E, Zivile K, Woodbury NW (2006) Signaling aptamers created using fluorescent nucleotide analogues. Anal Chem 78:6484–6489
12. Li JJ, Fang X, Tan W (2002) Molecular aptamer beacons for real-time protein recognition. Biochem Biophys Res Comm 292:31–40
13. Morse DP (2007) Direct selection of RNA beacon aptamers. Biochem Biophys Res Comm 359:94–101
14. Nutiu R, Li Y (2003) Structure switching signaling aptamers. J Am Chem Soc 125:4771–4778
15. Rajendran M, Ellington AD (2003) *In vitro* selection of molecular beacons. Nucleic Acids Res 31:5700–5713
16. Bruno JG, Ulvick SJ, Uzzell GL, Tabb JS, Valdes ER, Batt CA (2001) Novel immuno-FRET assay method for *Bacillus* spores and *E. coli* O157:H7. Biochem Biophys Res Comm 287:875–880

17. Anderson JP, Angerer B, Loeb LA (2005) Incorporation of reporter-labeled nucleotides by DNA polymerases. BioTechniques 38:257–264
18. Lacenere CJ, Garg NK, Stoltz BM, Quake SR (2006) Effects of a modified dye-labeled nucleotide spacer arm on incorporation by thermophilic DNA polymerases. Nucleosides Nucleotides Nucleic Acids 25:9–15
19. Zhu Z, Chao J, Yu H, Waggoner AS (1994) Directly labeled DNA probes using fluorescent nucleotides with different length linkers. Nucleic Acids Res 22:3418–3422
20. Crameri A, Stemmer WPC (1993) 10^{20}-Fold aptamer library amplification without gel purification. Nucleic Acids Res 21:4410
21. Hofacker IL (2003) Vienna RNA secondary structure server. Nucleic Acids Res 31:3429–3431
22. SantaLucia J (1998) A unified view of polymer, dumbbell, and oligonucleotide DNA nearest-neighbor thermodynamics. Proc Natl Acad Sci USA 95:1460–1465
23. Gouda H, Kuntz ID, Case DA, Kollman PA (2003) Free energy calculations for theophyllin binding to an RNA aptamer: comparison of MM-PBSA and thermodynamic integration methods. Biopolymers 68:16–34
24. Trubetskoy VS, Hagstrom JE, Budker VG (2002) Self-quenched covalent fluorescent dye-nucleic acid conjugates as polymeric substrates for enzymatic nuclease assays. Anal Biochem 300:22–26
25. Trubetskoy VS, Wolff JA, Budker VG (2003) The role of a microscopic colloidally stabilized phase in solubilizing oligomine-condensed DNA complexes. Biophys J 84:1124–1130
26. Hofkens J, Cotlet M, Vosch T, Tinnefeld P, Weston KD, Ego C, Grimsdale A, Müllen K, Beljonne D, Bredas JL, Jordens S, Schweitzer G, Sauer M, De Schryver F (2003) Revealing competitive Förster-type resonance energy-transfer pathways in single bichromophoric molecules. Proc Natl Acad Sci USA 100:13146–13151
27. Berlier JE, Rothe A, Buller G, Bradford J, Gray DR, Filanoski BJ, Telford WG, Yue S, Liu J, Cheung CY, Chang W, Hirsch JD, Beecham JM, Haugland RP, Haugland RP (2003) Quantitative comparison of long-wavelength Alexa Fluor dyes to Cy dyes: fluorescence of the dyes and their bioconjugates. J Histochem Cytochem 51:1699–1712
28. Nazarenko I, Pires R, Lowe B, Obaidy M, Rachtchian A (2002) Effect of primary and secondary structure of oligodeoxyribonucleotides on the fluorescent properties of conjugated dyes. Nucleic Acids Res 30:2089–2195
29. Unruh JR, Gokulrangan G, Lushington GH, Johnson CK, Wilson GS (2005) Orientational dynamics and dye-DNA interactions in a dye-labeled DNA aptamer. Biophys J 88:3455–3465
30. Marras SAE, Kramer FR, Tyagi S (2002) Efficiencies of fluorescence resonance energy transfer and contact-mediated quenching in oligonucleotide probes. Nucleic Acids Res 30: e122–e130
31. Heleg-Shabtai V, Gratziany N, Liron Z (2006) Separation and detection of VX and its methylphosphonic acid degradation products on a microchip using indirect laser-induced fluorescence. Electrophoresis 27:1996–2001
32. Corry B, Jayatilaka D, Rigby P (2005) A flexible approach to the calculation of resonance energy transfer efficiency between multiple donors and acceptors in complex geometries. Biophys J 89:3822–3836